Microsyst Technol (2013) 19:179–186
DOI 10.1007/s00542-012-1653-3

TECHNICAL PAPER

Ultra high aspect ratio penetrating metal microelectrodes for biomedical applications

Abishek B. Kamaraj · Murali M. Sundaram · Ronnie Mathew

Received: 6 April 2012 / Accepted: 10 August 2012 / Published online: 30 August 2012

Abstract Studying the functioning of the brain through the use of penetrating microelectrodes has revolutionized our understanding of the brain and has the potential to treat physical conditions such as the aftermath of a stroke, disease or other neural problems. Cochlear implant electrodes have transformed the lives of people who were suffering from cochlear auditory disorders. However, limitations of manufacturing procedures restrict the choice of work materials to mostly silicon based materials, and biocompatibility issues have constrained the extensive use of these devices. Metal microelectrodes can absolve this limitation and enable extensive study of the neural centers. In this paper we report the fabrication of tungsten penetrating microelectrodes using electrochemical machining. Ultra high aspect ratio penetrating metal microelectrodes with diameters 10 μm and below, with surface roughness (Ra) values in the range of 300–500 nm, have been fabricated by electrochemical machining process. Details regarding the fabrication process and a mathematical model developed for the electrochemical machining process are discussed in this paper.

1 Introduction

Penetrating microelectrode neural implants have been one of the main techniques used to understand how the brain processes information to sense and control body functions (Jensen et al. 2006).These devices allow direct and selective recording and stimulation of neural tissue which aids in the understanding of the neurophysiological processes in the human brain (McCarthy et al. 2011; Bak et al. 1990). From rats to monkeys, these microelectrodes have been used to control neuroprostheses through chronically implanted cortical electrodes, which sampled the extracellular potentials of the neuron (Taniguchi et al. 2007). Penetrating microelectrodes have also been used in auditory brain stem implants for the treatment and understanding of hearing related disorders (Schwartz et al. 2008; Spelman 1999). The diameter of these electrodes needs to be small in order to minimize the damage to neural tissue during the process of penetration. A smaller diameter of the electrode is also desirable due to lower penetrating forces associated with these devices (Jensen et al. 2006).

Advances in micro fabrication techniques, material sciences, and electronics have fueled a steady advancement in the development of these implantable microelectrodes for reliable and stable long-term monitoring of neuronal activities from the brain (Lee et al. 2004; Rousche et al. 2001). Many different materials have been explored for making multifunctional neural interfaces. Among the different materials, silicon has thus far been the most widely investigated material due to the ease of manufacturing enabled by the bulk manufacturing processes. However, there are questions regarding long-term stability with silicon-based implants, especially when considering that the brain is continuously under micro-motion that induces strain between the brain tissue and the implanted electrode. This promotes chronic injury and glial scarring locally around the implant site, thus causing concern for long-term safety and functional stability of the implanted device. Another significant drawback of the silicon based neural implants is its tendency to buckle. Buckling strength is an important mechanical characteristic of the penetrating microelectrode for neural interfaces. High buckling strength results in

A. B. Kamaraj · M. M. Sundaram (✉) · R. Mathew
Micro and Nano Manufacturing Laboratory, School of Dynamic Systems, University of Cincinnati, Cincinnati, OH, USA
e-mail: murali.sundaram@uc.edu

higher resistance to bending during insertion into the brain. But the small cross-sectional area and high aspect ratio of the microelectrode gives it an intrinsically low buckling strength, which becomes the main cause of failure for such devices. In order for a microelectrode to be directly inserted into the brain, its buckling strength must be high enough to withstand forces required to penetrate brain tissue and overcome the friction applied on the moving probe during insertion. Being brittle, solid silicon is prone to buckling which can result in serious tissue damage and neural disorders. This tendency to buckle is one limiting factor restricting the length of the microelectrode (Najafi et al. 1990). Longer electrodes provide access to subcortical structures which help in the study of neural processing networks such as corticothalamic loops (Nicolelis and Shuler 2001). The realization of the true potential of these devices has been hindered by these limiting factors in silicon microelectrodes.

Metal microelectrodes offer considerable advantages over silicon microelectrodes as they do not fail in brittle mode lowering the chance of catastrophic failure (McCarthy et al. 2011). Also, higher buckling strength permits the usage of slender high aspect ratio microelectrodes. The microelectrodes can be inserted into neural tissue without buckling and are easily manipulated into arrays. Metal microelectrodes that have been used for neural implants include tungsten (Patrick et al. 2008), and titanium (Droge et al. 1986). Commercial microelectrode arrays, as well as many noncommercial arrays, are made with tungsten microelectrodes. The strength, rigidity, and recording properties of tungsten microelectrodes make them desirable for intracortical applications (Patrick et al. 2011). Tungsten microelectrodes have also been used to study the activities of limb and facial peripheral nerves on conscious human subjects (Navarro et al. 2005). Studies show that although tungsten is prone to corrosion within biological systems it does not seem to be having any significant toxic effect on the metabolic rates (Peuster 2003). Current methods for fabrication of metal microelectrode neural implants are based on silicon substrate based microfabrication techniques which use electroplating techniques (Frazier et al. 1993). These techniques are limited only to a limited number of materials like nickel, gold, and silver. Another technique used in the manufacturing of such microelectrodes is chemical etching. In this technique metal wire tips are chemically etched to produce conical tips which act as recording sites (Takahashi et al. 2005). This technique can only be used for sharpening of the electrode and the actual microelectrode needs to be fabricated using another process. Titanium microelectrodes were manufactured using a combination process of chemical vapor deposition and silicon based photolithography (McCarthy et al. 2011). This complex method is a more expensive approach and the fabricated electrode had variations in thickness, as high as 4 μm. High aspect ratio electrodes have also been produced using wire electrodischarge process (WEDM) and micro grinding process (Ohmori et al. 2007; Jahan et al. 2010; Lim et al. 2003; Uhlmann et al. 2008). The WEDM process produces microelectrodes which have a rough finish with Ra values around 1–2 μm (Jahan et al. 2010). Micro grinding can produce microelectrodes with a very smooth finish with Ra values ranging from 0.1 to 0.7 μm (Ohmori et al. 2007). The drawback of micro grinding is that it is tough to scale up this process for mass production. Thus, it is essential that a process that is simple, precise, scalable, and able to produce metal microelectrodes with smooth finish is needed.

Electrochemical machining (ECM) is an alternative microfabrication technique that can be used to make these neural interfaces. ECM has many advantages over other traditional machining processes. Some of the advantages are its applicability regardless of material hardness, no tool wear, high material removal rate, smooth and bright surface, and the production of components of complex geometry (Sundaram and Rajurkar 2010). Pulse electrochemical micromachining (PECMM) is a variation of ECM for the micro scale fabrication, where a pulsed power is used instead of DC current. PECMM leads to higher machining accuracy, better process stability and suitability for control. These advantages are due to the improved electrolyte flow condition in the interelectrode gap, enhanced localization of anodic dissolution, and small and stable gaps found in PECMM (Rajurkar et al. 1993; Schuster et al. 2000). The PECMM technique discussed in this paper can be used to produce ultra high aspect ratio electrodes unlike the chemical etching techniques which give conical electrodes. High aspect ratio of these electrodes helps in minimizing the tissue damage during the insertion of these electrodes. The lower insertion forces due to the smaller diameter of these electrodes also aid in the reduction of tissue damage and increases the robustness of the electrodes by reducing the chances of buckling (HajjHassan et al. 2008). The non-contact nature of electrochemical machining poses challenges in ensuring machining accuracy and process control. This can be overcome with the development of a model, as described in Sect. 3 of this paper, for predicting the process parameters required to get the microelectrode with the desired size.

There have been a number of studies about the brain tissue and microelectrode interaction that provide a basis for understanding insertion forces in the human brain (Lee et al. 2004; Howard et al. 1999; Moon et al. 2003). A typical force characteristic while penetrating into a rat cerebral cortex was studied by Jensen et al. (2006) and reported a maximum penetrating force of 1.15 ± 0.51 mN

for 150 μm diameter microelectrodes (Jensen et al. 2006). The same study showed that smaller microelectrodes result in smaller penetration force. The maximum penetration force for a 28 × 38 μm rectangular electrode was about 0.48 ± 0.18 mN. This shows that smaller microelectrodes only need lower penetrating forces which helps in reducing the damage to surrounding tissues. Lower penetrating forces also help in reducing the chance of these electrodes failing due to buckling.

In this paper the finite element analysis (FEA) has been used to determine the diameter of the tungsten microelectrode that can handle the penetrating forces described in literature, without buckling. A mathematical model was developed to predict the process parameters required to fabricate the tungsten microelectrode with the diameter suggested by the FEA. Experimental verification of the model and the fabrication of ultra high aspect ratio microelectrodes are described subsequently.

2 Finite element analysis of tungsten microelectrode

A finite element method (FEM) based buckling analysis was performed to determine the minimum diameter of the tungsten microelectrode that can withstand the penetrating forces without buckling. Commercial FEM software ANSYS© was used in this eigenvalue buckling analysis (ANSYS 2010). Eigenvalue buckling analysis gives the theoretical buckling strength based on the classical eulerian approach (Yaghi et al. 2011). The buckling problem is formulated in the FEM as an eigenvalue problem.

$$([K] + \lambda_i[S])\{\psi\}_i = \{0\} \quad (1)$$

where: [K] = stiffness matrix, [S] = stress stiffness matrix, λ_i = ith eigenvalue, ψ_i = ith eigenvector of displacements.

This is solved using the Block Lanczos eigenvalue extraction method. A block shifted Lanczos algorithm, as found in (Grimes et al. 1994) is the theoretical basis of the Eigen solver. Figure 1 gives the schematic representation of the buckling analysis of the microelectrode. The symmetry of the buckling behavior is invoked in the analysis and only half of the structure is modeled for the analysis. Table 1 gives the FEM parameters used in the analysis. Figure 2 gives the simulated deflection behavior of the microelectrode after application of the load, and the onset of buckling.

Using FEA it was found that, to overcome penetrating forces of 0.45 mN, the diameter of the tungsten microelectrode needs to be at least 10 μm. This value of force is experienced only on microelectrodes having a cross-section of 25 × 38 μm. As smaller cross-sections will encounter even lower forces (Jensen et al. 2006), FEM analysis reveals that the tungsten microelectrodes with diameters greater than 10 μm are capable of handling the penetrating forces involved during insertion into brain tissue. To establish the process parameters of ECM to fabricate microelectrodes of the size suggested by FEA, a mathematical model was developed as mentioned in the next section.

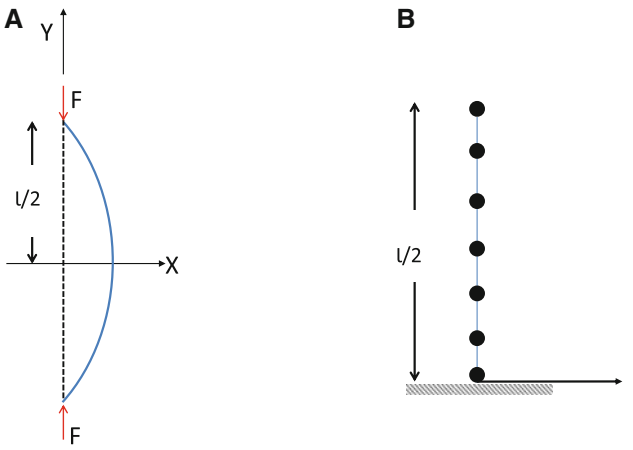

Fig. 1 Finite element analysis. **a** Schematic of loading of the microelectrode. The maximum F that was applied was 1mN divided into 5 load steps. **b** Finite element representation of half of the microelectrode (after symmetry conditions)

Table 1 Finite element analysis parameters

FEA parameter	Value
Element type	Beam 188
Material	Tungsten, isotropic
Analysis type	Eigenvalue buckling
Load	Unit load 1 N
Model	Ø10 μm, 2 mm long (l) microelectrode
No. of nodes	10
Young's modulus	411 GPa

Fig. 2 Deflection behavior of tungsten microelectrode at the onset of buckling (only half of the microelectrode has been represented)

3 Mathematical model for microelectrode fabrication

In order to establish the standard process parameters for the electrochemical machining process to produce tungsten electrodes with the desired diameter a mathematical model (Eq. 2) was developed to predict the anodic profile of microelectrode (Mathew and Sundaram 2012).

$$D_f = D_i - 2\left(\sqrt{S_0^2 + \frac{pW}{V} 2\eta\kappa_e k_v (U_0 - \Delta U) t_p} - S_0\right) \quad (2)$$

This model involves a system where the cathode is moving. The anode has an initial diameter D_i and a cathode of width W is kept at an initial interelectrode gap S_0. This model uses the interelectrode gap to formulate the final diameter of the tool D_f in terms of the various ECM parameters. In the case of the PECMM system shown in Fig. 3 with the stationary cathode this model needs to be modified to suit this system. The term W/V is the time spent by a part of the anode under the influence of the cathode. This is the same as the total machining time in the case of a wide stationary cathode. Thus,

$$\frac{W}{V} = T \quad (3)$$

where T is the total machining time. The resulting model is given in Eq. 4.

$$D_f = D_i - 2\left(\sqrt{S_0^2 + pT2\eta\kappa_e k_v (U_0 - \Delta U) t_p} - S_0\right) \quad (4)$$

where, η is the current efficiency of anodic dissolution (20 %), κ_e is the electrolyte conductivity (19 A/Vm), k_v is the volumetric electrochemical equivalent (1.65×10^{-11} m^3/As) S_0 is the interelectrode gap (0.15 mm), U_0 is the applied voltage (3 V), P is the pulse rate or frequency (66.6 Hz), t_p is the pulse on-time (5 ms), and ΔU is the over-potential value (0 V). Using the above model the experimental condition required for the desired size of microelectrode can be predicted precisely. Thus to obtain a Ø10 μm sized microelectrode starting with a Ø300 μm electrode, the required machining time T predicted is 515 s. The experimental verification of this model is discussed in the next section along with the general ECM procedure.

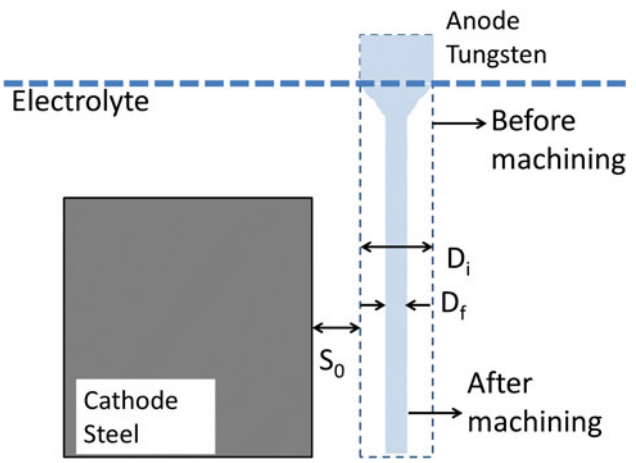

Fig. 3 Schematic of PECMM for model

4 Pulse electrochemical micromachining procedure

Electrochemical machining (ECM) is a nontraditional machining process in which material is removed by the mechanism of anodic dissolution in an electrolytic cell during an electrolysis process (Rajurkar et al. 1999). In this process, the part to be machined is made the anode while the tool that does the machining is made the cathode. The anodic dissolution rate which is the rate at which the anodic metal is removed depends on the electrochemical properties of the metal and the current applied (McGeough 1974). The cathode, or the tool, remains unaltered by the electrochemical machining process which gives ECM an edge over many other processes, as there is no tool wear or any other need to change the tool.

Pulse electrochemical micromachining (PECMM) is a variation of ECM in which a pulsed current is used as the power source for electrochemical micromachining. Pulse electrochemical micromachining (PECMM) provides an attractive alternative not only to ECM using continuous current, but also to many other traditional machining processes. The improved electrolyte flow condition in the interelectrode gap, enhanced localization of anodic dissolution, and small and stable gaps found in PECMM lead to higher dimensional accuracy, better process stability, relatively simpler tool design and better suitability for online process control (Rajurkar et al. 1993). Several studies have been conducted on the fabrication of microelectrodes using ECM (Zhang et al. 2007; Staemmler et al. 2008; Jain et al. 2012; Bhattacharyya et al. 2004; Choi et al. 2007). These electrodes were fabricated using conventional ECM. In this study, PECMM has been used along with reverse pulses in order to produce the microelectrodes with high aspect ratios needed for the neural implants.

The experimental setup is shown in Fig. 4. The electrolytic tank holding the cathode is filled with the electrolyte and is mounted on an XYZ stage which can provide the motion in the longitudinal, lateral, and axial directions. The spindle holding the anode feeds the anode in the vertical direction and rotates at a constant rate during the experiment. The power supply connects to both the anode and the cathode and provides the required current for machining. After the anode is positioned with respect to the cathode, the power supply is turned on and used at a constant current mode. The constant current mode enables

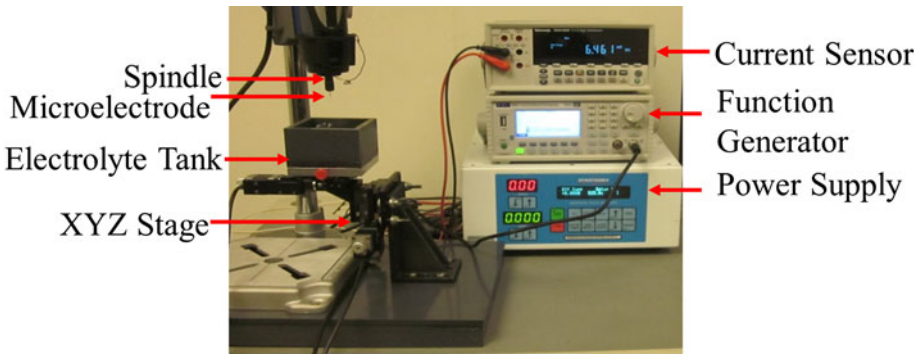

Fig. 4 Experimental Setup for PECMM of tungsten microelectrodes

Table 2 ECM parameters

Power supply	10 V DC
Anode	Tungsten rod of Ø300 μm
Cathode	0.5 mm thick stainless steel plate
Electrolyte	10 % wt. Sodium chloride solution
Average current	0.05 A
Pulse time	15 ms
Duty cycle	33 %
Spindle rotation	1000 rpm
Interelectrode gap	0.15 mm

the system to keep a fixed current and vary the voltage as the tool moves relatively to the cathode. The relative position between the anode and cathode is maintained at a gap of 0.15 mm. The experimental parameters used are given in Table 2.

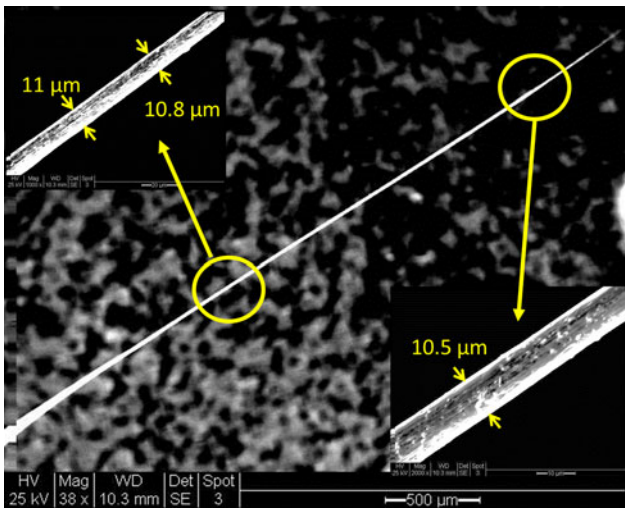

Fig. 5 SEM micrograph of fabricated tungsten microelectrode showing the variation of the diameter

5 Results and discussion

The mathematical model predicted that to obtain a microelectrode of diameter 10 μm the time for machining is 515 s. The experimental validation of the mathematical model was done by conducting experiments with the process parameters suggested by the mathematical model. This experiment was conducted three times to verify the repeatability and minimize variation due to experimental errors. The resulting microelectrode is given in Fig. 5. The diameter that was measured is the average value of the measured diameter at 3 different positions over the length of the microelectrode. The three microelectrodes had an average diameter of 10.5, 11 and 12 μm with standard deviation 0.35, 0.49 and 0.58 μm respectively. This shows that the mathematical model is capable of predicting the microelectrode profile within ± 2 μm except at the tip zone which is less than about 2 % of the total length of the electrode. While the size and shape of the electrodes have been found to have serious impacts on tissue damage, the recorded signals are not significantly affected similarly (Szarowski et al. 2003). Thus these variations fall within the acceptable range. It is also observed that the tip of the electrode (30 μm from the end) is slightly smaller than the rest of the electrode. The smaller tip is advantageous as it helps in penetration due to lower penetrating forces. The 3D noncontact confocal microscopic analysis showed that the microelectrodes have surface roughness (Ra) values in the range of 0.3–0.5 μm depending on the process conditions. The roughness was calculated on 3 different samples of the microelectrodes with a mean of 0.39 μm and standard deviation 0.09 μm. The vertical resolution of the microscope is 10 nm. Line scan of the 3D image data on the surface of the electrode was used to determine the roughness. The line length was approximately 800 μm along the surface of the electrode. A representative surface roughness measurement result is given in Fig. 6. The typical surface roughness value of a drawn tungsten rod with a diameter of 300 μm, which were used as the starting electrodes, is 8 μm. In comparison, silicon penetrating microelectrodes used as neural implants have surface roughness values around 1 μm (Szarowski et al. 2003). Surface texture is known to have an influence on the response of the tissue surrounding the implanted electrode

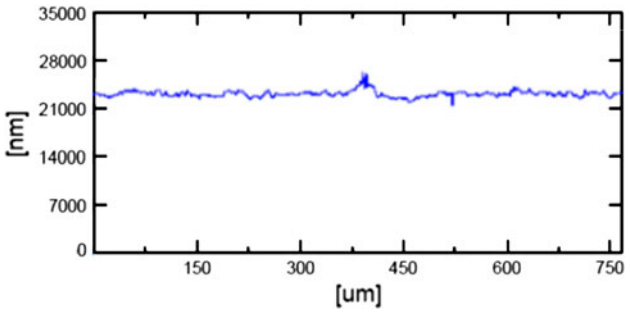

Fig. 6 Surface roughness measurement on microelectrode with sample length 800 μm (Ra = 0.31 μm)

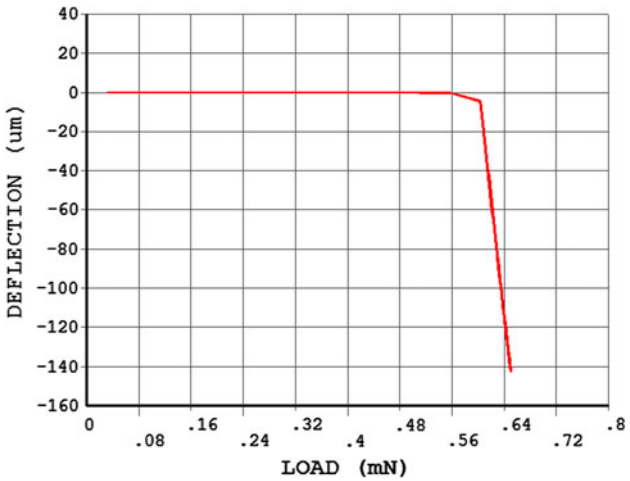

Fig. 7 Load deflection curve of Ø10.5 μm microelectrode showing onset of buckling at 0.56 mN

(Taylor and Gibbons 1983). A smooth surface lowers the chance of tissue regrowth on the electrode, which can interfere with the recorded signals. Near term signal recording (within 1 week of implant) is significantly affected by the surface finish with smooth finish giving improved results (Szarowski et al. 2003). Thus the surface finish produced by the PECMM process assumes significance and the low value of roughness (0.3 μm) indicates the suitability of these electrodes for this application.

The fabricated microelectrodes were again tested for their buckling behavior using FEA with the revised dimensions. The simulated buckling strength of the electrodes were 0.56, 0.69, 0.72 mN for the fabricated electrodes with diameters 10.5, 11 and 12 μm respectively. The load deflection curve for the Ø10.5 μm electrode giving its buckling behavior with increase in load is given in the Fig. 7. The onset of buckling is noticed with the huge increase in the deflection after the critical buckling load of 0.56 mN. These results again validate the robustness of the microelectrode.

These microelectrodes can be used as individual (single) penetrating microelectrodes to record single neuron signals

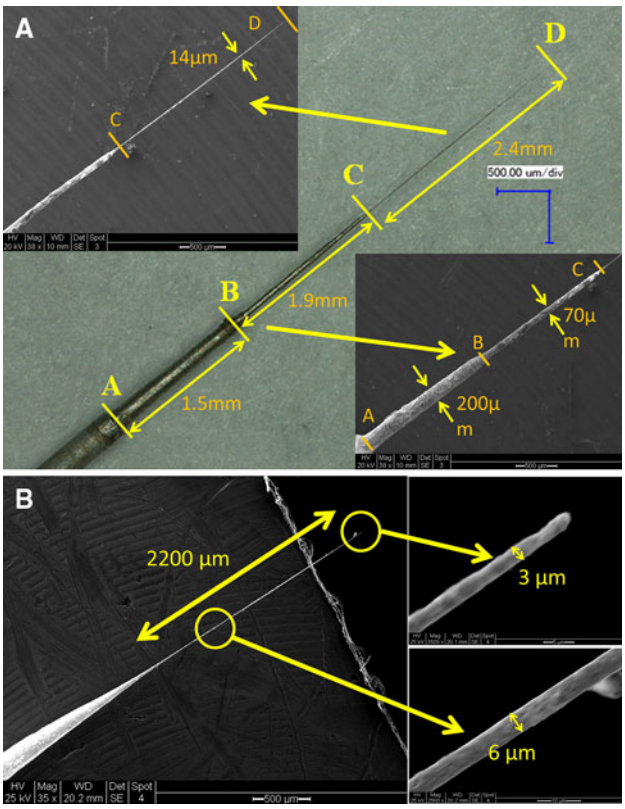

Fig. 8 High aspect ratio microelectrodes. **a** Stepped microelectrode of total length 5.8 mm with diameters of 200, 70 and 15 μm in the three sections. **b** Microelectrode with average Ø6 μm and tip Ø3 μm

or several of these electrodes can be combined into an array for monitoring neuron networks (Polikov et al. 2005). The metal microelectrode arrays currently in use range from 4 electrodes to 100 electrodes. These electrodes are arrayed using epoxy bonding materials. The opposite ends of the electrodes are connected to electrical connector pins which are connected to the signal analyzing circuitry that records the neural signals (Rousche et al. 2001).

This PECMM process is also capable of fabricating microelectrodes with varying shapes and sizes. Starting with a 300 μm tungsten rod, microelectrodes ranging from Ø50 to Ø2 μm can be produced (Fig. 8). The lengths of these high aspect ratio (up to 400) microelectrodes are in a range of 1 mm to 5 mm long, making them suitable for neural implants. Several microelectrodes can be produced simultaneously in a single electrolytic tank with a setup having provision to hold multiple rotating electrodes. This will enable the mass production of these electrodes.

6 Conclusion

This study establishes the feasibility of fabricating high aspect ratio, metal, microelectrodes using pulsed

electrochemical micromachining process. High aspect ratio of the order of 400 with diameters as small as 10 μm or less has been achieved in the fabrication of metal microelectrodes for biomedical applications such as neural and cochlear implants. A mathematical model to preselect the machining conditions for the desired electrode size given by FEA studies has also been developed. The model was verified experimentally and was found to predict the final diameter of the microelectrode to within ± 2 μm accuracy. Surface characterization of the microelectrodes suggests that the fabricated microelectrodes have preferable roughness values within the acceptable range for penetrating microelectrodes. The PEC-MM process thus designed for fabrication of penetrating microelectrodes is simple, precise, scalable and robust.

Acknowledgments Financial support provided by the National Science Foundation under Grant No CMMI–1120382, CBET-1239779 and by the University of Cincinnati under the URC Faculty Research Grant program is acknowledged. We thank Mr. Steve Volz of Carl Zeiss microscopy for the surface roughness measurement. The scanning electron microscopy facilities provided by the Advanced Material Characterization Center at the University of Cincinnati are acknowledged.

References

ANSYS (2010) Help system, buckling analysis guide. ANSYS® Acad Res Rel 121

Bak M, Girvin J, Hambrecht F, Kufta C, Loeb G, Schmidt E (1990) Visual sensations produced by intracortical microstimulation of the human occipital cortex. Med Biol Eng Comput 28(3): 257–259. doi:10.1007/bf02442682

Bhattacharyya B, Munda J, Malapati M (2004) Advancement in electrochemical micro-machining. Int J Mach Tools Manuf 44(15):1577–1589. doi:10.1016/j.ijmachtools.2004.06.006

Choi S, Ryu S, Choi D, Chu C (2007) Fabrication of WC micro-shaft by using electrochemical etching. Int J Adv Manuf Technol 31(7):682–687. doi:10.1007/s00170-005-0241-4

Droge MH, Gross GW, Hightower MH, Czisny LE (1986) Multi-electrode analysis of coordinated, multisite, rhythmic bursting in cultured CNS monolayer networks. J Neurosci 6(6):1583

Frazier AB, O'Brien DP, Allen MG (1993) Two dimensional metallic microelectrode arrays for extracellular stimulation and recording of neurons. In: Micro electro mechanical systems, 1993, MEMS '93, Proceedings an investigation of micro structures, sensors, actuators, machines and systems. IEEE pp 195–200

Grimes RG, Lewis JG, Simon HD (1994) A shifted block lanczos algorithm for solving sparse symmetric generalized eigenproblems. SIAM J Matrix Anal Appl 15(1):228–272

HajjHassan M, Chodavarapu V, Musallam S (2008) NeuroMEMS: neural probe microtechnologies. Sensors 8(10):6704–6726

Howard MA III, Abkes BA, Ollendieck MC, Noh MD, Ritter C, Gillies GT (1999) Measurement of the force required to move a neurosurgical probe through in vivo human brain tissue. Biomed Eng IEEE Trans 46(7):891–894. doi:10.1109/10.771205

Jahan MP, Rahman M, Wong YS, Fuhua L (2010) On-machine fabrication of high-aspect-ratio micro-electrodes and application in vibration-assisted micro-electrodischarge drilling of tungsten carbide. Proc Inst Mech Eng Part B J Eng Manuf 224(5):795–814. doi:10.1243/09544054jem1718

Jain VK, Kalia S, Sidpara A, Kulkarni VN (2012) Fabrication of micro-features and micro-tools using electrochemical micromachining. Int J Adv Manuf Technol:1–9. doi:10.1007/s00170-012-4088-1

Jensen W, Yoshida K, Hofmann UG (2006) In vivo implant mechanics of flexible, silicon-based ACREO microelectrode arrays in rat cerebral cortex. Biomed Eng IEEE Trans 53(5): 934–940. doi:10.1109/tbme.2006.872824

Lee K, Singh A, He J, Massia S, Kim B, Raupp G (2004) Polyimide based neural implants with stiffness improvement. Sens Actuators B Chem 102(1):67–72. doi:10.1016/j.snb.2003.10.018

Lim HS, Wong YS, Rahman M, Edwin Lee MK (2003) A study on the machining of high-aspect ratio micro-structures using micro-EDM. J Mater Process Technol 140(1–3):318–325. doi:10.1016/s0924-0136(03)00760-x

Mathew R, Sundaram MM (2012) Modeling and fabrication of micro tools by pulsed electrochemical machining. J Mater Process Technol 212(7):1567–1572. doi:10.1016/j.jmatprotec.2012.03.004

McCarthy PT, Otto KJ, Rao MP (2011) Robust penetrating microelectrodes for neural interfaces realized by titanium micromachining. Biomed Microdev 13(3):503–515. doi:10.1007/s10544-011-9519-5

McGeough JA (1974) Principles of electrochemical machining. Chapman and Hall, London

Moon T, Ghovanloo M, Kipke DR (2003) Buckling strength of coated and uncoated silicon microelectrodes, vol. 1942. In: Engineering in medicine and biology society, 2003. Proceedings of the 25th annual international Conference of the IEEE, pp 1944–1947. doi: 10.1109/iembs.2003.1279821

Najafi K, Ji J, Wise KD (1990) Scaling limitations of silicon multichannel recording probes. Biomed Eng IEEE Trans 37(1): 1–11

Navarro X, Krueger TB, Lago N, Micera S, Stieglitz T, Dario P (2005) A critical review of interfaces with the peripheral nervous system for the control of neuroprostheses and hybrid bionic systems. J Peripher Nerv Syst 10(3):229–258. doi:10.1111/j.1085-9489.2005.10303.x

Nicolelis MAL, Shuler M (2001) Chapter 7 Thalamocortical and corticocortical interactions in the somatosensory system. In: Nicolelis MAL (ed) Progress in brain research, vol 130. Elsevier, Amsterdam, pp 89–110

Ohmori H, Katahira K, Naruse T, Uehara Y, Nakao A, Mizutani M (2007) Microscopic grinding effects on fabrication of ultra-fine micro tools. CIRP Ann Manuf Technol 56(1):569–572. doi:10.1016/j.cirp.2007.05.136

Patrick E, Sankar V, Rowe W, Yen SF, Sanchez JC, Nishida T (2008) Flexible polymer substrate and tungsten microelectrode array for an implantable neural recording system. In: IEEE, pp 3158–3161

Patrick E, Orazem ME, Sanchez JC, Nishida T (2011) Corrosion of tungsten microelectrodes used in neural recording applications. J Neurosci Methods 198(2):158–171. doi:10.1016/j.jneumeth.2011.03.012

Peuster M (2003) Biocompatibility of corroding tungsten coils: in vitro assessment of degradation kinetics and cytotoxicity on human cells. Biomaterials 24(22):4057–4061. doi:10.1016/s0142-9612(03)00274-6

Polikov VS, Tresco PA, Reichert WM (2005) Response of brain tissue to chronically implanted neural electrodes. J Neurosci Methods 148(1):1–18. doi:10.1016/j.jneumeth.2005.08.015

Rajurkar KP, Kozak J, Wei B, McGeough JA (1993) Study of pulse electrochemical machining characteristics. CIRP Ann Manuf Technol 42(1):231–234. doi:10.1016/s0007-8506(07)62432-9

Rajurkar KP, Zhu D, McGeough JA, Kozak J, De Silva A (1999) New developments in electro-chemical machining. CIRP Ann Manuf Technol 48(2):567–579. doi:10.1016/s0007-8506(07)63235-1

Rousche PJ, Pellinen DS, Pivin DP Jr, Williams JC, Vetter RJ, kirke DR (2001) Flexible polyimide-based intracortical electrode arrays with bioactive capability. Biomed Eng IEEE Trans 48(3):361–371. doi:10.1109/10.914800

Schuster R, Kirchner V, Allongue P, Ertl G (2000) Electrochemical micromachining. Science 289(5476):98–101. doi:10.1126/science.289.5476.98

Schwartz MS, Otto SR, Shannon RV, Hitselberger WE, Brackmann DE (2008) Auditory brainstem implants. Neurotherapeutics 5(1):128–136. doi:10.1016/j.nurt.2007.10.068

Spelman FA (1999) The past, present, and future of cochlear prostheses. Eng Med Biol Mag IEEE 18(3):27–33

Staemmler L, Hofmann K, Kück H (2008) Hybrid tooling by a combination of high speed cutting and electrochemical milling with ultrashort voltage pulses. Microsyst Technol 14(2):249–254. doi:10.1007/s00542-007-0423-0

Sundaram MM, Rajurkar K (2010) Electrical and electrochemical processes. In: Intelligent energy field manufacturing. CRC Press, pp 173–212. doi:10.1201/EBK1420071016-c6

Szarowski DH, Andersen MD, Retterer S, Spence AJ, Isaacson M, Craighead HG, Turner JN, Shain W (2003) Brain responses to micro-machined silicon devices. Brain Res 983(1–2):23–35. doi:10.1016/s0006-8993(03)03023-3

Takahashi H, Suzurikawa J, Nakao M, Mase F, Kaga K (2005) Easy-to-prepare assembly array of tungsten microelectrodes. Biomed Eng IEEE Trans 52(5):952–956. doi:10.1109/tbme.2005.845224

Taniguchi N, Suzuki T, Mabuchi K Biocompatibility of wire electrodes improved by MPC polymer coating. In: Neural engineering, 2007. CNE '07. 3rd International conference on IEEE/EMBS, pp 122–125

Taylor SR, Gibbons DF (1983) Effect of surface texture on the soft tissue response to polymer implants. J Biomed Mater Res 17(2):205–227. doi:10.1002/jbm.820170202

Uhlmann E, Piltz S, Oberschmidt D (2008) Machining of micro rotational parts by wire electrical discharge grinding. Prod Eng 2(3):227–233. doi:10.1007/s11740-008-0094-4

Yaghi AH, Hyde TH, Becker AA, Sun W (2011) Finite element simulation of welded P91 steel pipe undergoing post-weld heat treatment. Sci Technol Weld Join 16 (Compendex):232–238

Zhang Z, Zhu D, Qu N, Wang M (2007) Theoretical and experimental investigation on electrochemical micromachining. Microsyst Technol 13(7):607–612. doi:10.1007/s00542-006-0369-7